Cell Adhesion and Communication, 1999, Vol. 7, No. 3, pp. 167–181
Reprints available directly from the publisher
Photocopying permitted by license only

Mutational Analysis of MAdCAM-1/$\alpha 4\beta 7$ Interactions Reveals Significant Binding Determinants in Both the First and Second Immunoglobulin Domains

NANCY GREEN[a], JOSH ROSEBROOK[a], NANCY COCHRAN[a], KEMIN TAN[b], JIA-HUAI WANG[b], TIMOTHY A. SPRINGER[c] and MICHAEL J. BRISKIN[a,*]

[a]*LeukoSite Inc., 215 First St., Cambridge, MA 02142, USA;* [b]*Laboratory of Immunobiology, Dana-Farber Cancer Institute and Children's Hospital, Harvard Medical School, 44 Binney Street, Boston, MA 02115, USA;* [c]*The Center for Blood Research and Department of Pathology, Harvard Medical School, 200 Longwood Avenue, Boston, MA 02115, USA*

(Received 14 April 1998)

The selective emigration of blood born leukocytes into tissues is mediated, in part by interactions of Ig-like cell adhesion molecules (IgCAMs) expressed on vascular endothelium and their cognate ligands, the leukocyte integrins. Within mucosal lymphoid tissues and gastrointestinal sites the mucosal vascular addressin, MAdCAM-1 is the predominant IgCAM, mediating specific lymphocyte homing via interactions with its ligand on lymphocytes, the integrin $\alpha 4\beta 7$. Previous studies have shown that an essential binding motif resides in the first Ig domain of all IgCAMs, containing an acidic residue (D or E) preceded by an aliphatic residue (L or I) that resides in strand C or the CD loop. However, domain swap experiments with MAdCAM-1 and VCAM-1 have shown a requirement for both Ig domains 1 and 2 for efficient integrin binding. We describe the use of chimeric MAdCAM-1/VCAM-1 receptors and point mutations in MAdCAM-1 to define other sites that are required for binding to the integrin $\alpha 4\beta 7$. We find that, in addition to critical CD loop residues, other regions in both domain one and two contribute to MAdCAM-1/$\alpha 4\beta 7$ interactions, including a buried arginine residue in the F strand of domain one and several acidic residues in a highly extended DE ribbon in domain 2. These mutations, when placed in the recently solved crystal structure of human MAdCAM-1 give insight into the integrin binding preference of this unique receptor.

Keywords: MAdCAM-1, VCAM-1, ICAM-1, IgCAM, mAb, MEM, FCS

Abbreviations: MAdCAM-1, Mucosal addressin cell adhesion molecule-1; VCAM-1, Vascular cell adhesion molecule-1; ICAM-1, IgCAM, Immunoglobulin like cell adhesion molecules; mAb, monoclonal antibody; MEM, minimal essential media; FCS, fetal calf serum

* Corresponding author. Tel.: 617 621 9350, ext. 1390. Fax: 617 621 9380. E-mail: Mike_Briskin@LeukoSite.com.

INTRODUCTION

Leukocyte trafficking requires multiple adhesive and activating events which, in combination, contribute to remarkable tissue specificity in the homing of lymphocyte subsets (Butcher, 1991; Picker and Butcher, 1992; Springer, 1994). Within intestinal lymphoid tissues and gastrointestinal organs, selectivity is largely governed by the expression of the mucosal vascular addressin, MAdCAM-1 (Berlin *et al.*, 1993; Briskin *et al.*, 1993; 1997; Shyjan *et al.*, 1996; Streeter *et al.*, 1988). MAdCAM-1 is a multi-domain molecule consisting of two amino-terminal Ig-like domains followed by mucin-like sequences and, in the case of murine MAdCAM-1, a membrane proximal Ig domain with homology to IgA (Briskin *et al.*, 1993; Shyjan *et al.*, 1996). The two amino terminal Ig domains display homology to other vascular Ig-like adhesion receptors, namely, ICAM-1 and VCAM-1 and are all functionally related by their interactions with integrin ligands expressed on various classes of leukocytes (Picker and Butcher, 1992; Springer, 1994). In the case of MAdCAM-1, its sole integrin ligand is $\alpha4\beta7$, an integrin that is expressed on sub-populations of mucosal homing lymphocytes (Berlin *et al.*, 1993; Erle *et al.*, 1994; Rott *et al.*, 1996; Schweighoffer *et al.*, 1993). VCAM-1 is functionally related to MAdCAM-1 in that it also binds the $\alpha4$ integrins: $\alpha4\beta1$ is a dominant ligand for VCAM-1, but VCAM-1 can also interact with $\alpha4\beta7$, although this appears to be a lower affinity interaction as activation is required (Ruegg *et al.*, 1992).

These findings have led to the proposition that the expression of $\alpha4\beta1$ versus $\alpha4\beta7$ integrins on lymphocytes represents a major point of delineation between peripheral and gastrointestinal immune responses (Rott *et al.*, 1996; Williams and Butcher, 1997). Along these lines, it has recently been demonstrated that mAbs to $\beta7$ or MAdCAM-1 show therapeutic efficacy in murine models of inflammatory bowel disease (IBD) (Picarella *et al.*, 1997). Furthermore, the success of anti-$\alpha4\beta7$ mAb ACT-1 therapy in alleviating symptoms in chronically colitic cotton-top tamarins (CTTs) demonstrates the therapeutic benefit to be gained by selective anti-MAdCAM-1/$\alpha4\beta7$ intervention (Hesterberg *et al.*, 1996).

Human MAdCAM-1, while functionally identical to its murine counterpart, is significantly different in several ways. The two N-terminal Ig domains, while the most conserved region of the molecules, are only 57% identical at the amino acid level (Shyjan *et al.*, 1996). Previous domain swapping experiments have demonstrated the importance of both the first and second Ig domains of murine MAdCAM-1 in binding $\alpha4\beta7$ while site directed mutagenesis has shown that a site in the first Ig domain is essential for binding $\alpha4\beta7$ (Briskin *et al.*, 1996; Newham *et al.*, 1997; Viney *et al.*, 1997). This site shows homology to a number of short, acidic peptide motifs related to the tripeptide sequences RGD and LDV present in fibronectin (Ruoslahti, 1991) which resides in all IgCAMs as well (Briskin *et al.*, 1993). This motif has been shown to reside on an exposed CD loop in the crystal structure of both MAdCAM-1 and VCAM-1 but lies on a flat surface on the end of the C strands in ICAM and 2 (Casasnovas *et al.*, 1997; 1998; Jones *et al.*, 1995; Tan *et al.*, 1998; Wang *et al.*, 1995). While these differences may yield some explanation as to the unique binding specificity of these receptors, swapping these loop regions either led to a lack of expression or demonstrated no change in integrin specificity, and suggests that regions outside of this conserved sequence are important for selective integrin binding (Newham *et al.*, 1997; Osborn *et al.*, 1994). In this study, we make use of chimeric MAdCAM-1/VCAM-1 receptors to identify sites important for $\alpha4\beta7$ binding and show that these regions extend across Ig domains 1 and 2. In addition, we have made a series of point mutations that emphasize the importance of a unique motif within the second domain of human MAdCAM-1. The mutational results are interpreted with the recently solved crystal structure of human MAdCAM-1 (Tan *et al.*, 1998).

MATERIAL AND METHODS

Cell Lines and mAbs

Plasmids for all constructs or for controls were PSV-SPORT-1 (Gibco/BRL, Gaithersburg, MD) or pcDNA3 or pcDNA3.1 (Invitrogen, San Diego, CA), seven domain human VCAM-1 (Polte *et al.*, 1990) in pcDNA3 (pCD3VCAM), and human MAdCAM-1 in pcDNA3 (pCDhuMAd4) (Shyjan *et al.*, 1996), soluble IgG–MAdCAM-1 chimera (Tidswell *et al.*, 1997). Monoclonal antibodies used were anti-human VCAM-1 2G7 (Graber *et al.*, 1990) and commercially available anti-VCAM-1 mAbs (Immunotech, Westbrook, ME, Bectin Dickenson, San Jose, CA and Novacastra, Burlingame, CA), anti-murine $\beta 7$ FIB 504 (Andrew *et al.*, 1994), anti-human $\alpha 4\beta 7$ ACT-1 (Lazarovits *et al.*, 1984), anti-human integrin $\beta 1$ (CD29, Becton Dickinson, San Jose, CA) and murine IgG1 and rat IgG2A as irrelevant controls. A panel of anti-human MAdCAM-1 mAbs included 10G3, 5E10, 7H12, 8C1, 10A6, 3b11, 9G12, 1E10, 1E5 and 4G5 (Briskin *et al.*, 1997). Cell lines used for functional adhesion assays were CHO/P (Heffernan and Dennis, 1991), RPMI 8866 (Erle *et al.*, 1994) and Ramos (American Type Tissue Culture Collection).

Construction of Chimeric Receptors and Mutagenesis

A truncated version of VCAM-1 with a deletion of the second VLA-4 binding site, defined by domains 4–6 was constructed by PCR. Domains 1–3 of 7 domain VCAM-1 were generated using the forward amplification primer 5′CGATGCGGCCGCCCACCATGCCTGGGAAGA3′ and the reverse amplification primer 5′GATCGAGCTCCACCTCTTTTCTGTTTTTCCCAATCAAATTAACTCC3′ and Ig domain 7 with the Tm and Cyto domains with forward amplification primer GATCGAGCTCATTATCCAAGTTACTGAC and reverse amplification primer 5′GATCGGTACCGCATTAGCTACACTTTTGATTTCTGTGC3′. These two fragments were ligated together into the vector pcDNA3.1 (Invitrogen, San Diego, CA). Domain swaps between MAdCAM-1 and VCAM-1 were facilitated by the use of a BAM H1 site at NT 450 in VCAM-1 between K93 and D94. A BAM H1 site was engineered in MAdCAM-1 to generate a fragment from the start codon using a forward amplification primer (MAd 5′Kpn), 5′GGGGTACCACCATGGATTTCGGACTGGGCC3′ and a reverse amplification primer 5′GCTGGATCCACGGTCAGCTGGTCCGG3′ designated DS20. The domain 1 fragment digested with Kpn-1 and BAM H1 was joined to a BAM H1 to XHO 1 restriction fragment of VCAM-1 encompassing domains 2, 3 and 7 along with the Tm and Cyto regions and subcloned into the vector pcDNA3.1 (Invitrogen) to generate M1V2,3,7. Domain 1 of VCAM-1 was excised with Not 1 and Bam H1 and joined to a Bam H1/Xho 1 fragment of MAdCAM-1 lacking domain 1 made with the forward amplification primer (DS23) 5′GGGGATCCAGCAGCCCTGGTGCCT3′ (which changed S99 to the corresponding D94 in domain 2 of VCAM-1) and the reverse amplification primer (DS7) 5′GGGCTCGAGAAAGGCTGGCCACTCAGG3′. Exchange of C′E loop in domain two of VCAM-1 for the DE loop in domain two of MAdCAM-1 was facilitated by the use of a PCR primer which created restriction sites (while introducing silent mutations) before the loop (for MAdCAM-1) and after the loop for VCAM-1. For example the VCAM C′E loop was engineered into MAdCAM-1 by use of the forward amplification primer:

5′CC CAA GCT TTG GAG GAT GCA GCA GAC AGG AAG TCC CTG GAA ACC CTG

Hind III VCAM C′E MAdCAM-1

TTC AGG GTG ACA GAG C3′

in conjunction with reverse amplification primer DS7. The primer MAd5′Kpn was used in conjunction with the reverse amplification primer 5′CCCAAAGCTTGCGCCCCCTCCAG3′ to engineer the HIND III site for the 5′ fragment. These fragments were subsequently ligated into pCDNA3.1. Similar approaches were used for grafting the MAdCAM-1 DE ribbon into VCAM-1.

Point mutants of the MAdCAM-1-Ig construct were made using the QuikChange Mutagenesis Kit and *Pfu* DNA polymerase (Stratagene, La Jolla, CA). Alanine was substituted in all cases except for additional CD Loop mutations, L45R and D46E. Mutagenic primers contained 10–16 bp of template sequence adjacent to the changed bases (e.g., the sense primer for D46A reads 5′-CGG GGC CTG GcC ACC AGC CTG G-3′). However, primers designed to create multiple mutations were accompanied by as many as 21 bp of adjacent sequence (as in the VMCD primer below). The five residue MAdCAM CD loop swapped into the membrane form of VCAM also employed this method. The sense VMCD primer was 5′-CCA TTT TTC TCT TGG AGA ACC ggG tTA GAT AcT tCA CTG AAT GGG AAG GTG ACG-3′. All mutated regions, domain and loop swaps were sequenced using the ThermoSequenase Kit (Amersham Life Science, Inc., Cleveland, OH). A complete list of mutagenic primers for all constructs made are available upon request.

Adhesion Assays

CHO/P cells were plated at 1×10^6 cells/10 cm tissue culture plate (Falcon), and incubated overnight at 37°C. Media was removed and cells were rinsed with 2 ml Opti-MEM 1 (GIBCO, Life technologies, Gaithersburg, MD). Lipofectamine Reagent (GIBCO) at a concentration of 60 µl/plate was mixed with 10 µg plasmid DNA in 1.6 ml Opti-MEM 1, incubated 25 min at ambient temperature and subsequently added to cells with 6.4 ml additional Opti-MEM 1. After 2.25 h incubation at 37°C, equal volume (8 ml) of alpha-MEM/20% fetal bovine serum (FBS) (GIBCO) was added to cells for overnight incubation. The following morning, media was changed to standard media (MEM-α/10% FCS) and late the same day cells were replated at a density of 25,000 cells/well in 48-well plates for adhesion assays. Cells not used in the 48-well plates were returned to the 10 cm plates for FACS analysis.

The following day, cell adhesion assays were performed as previously described (Briskin *et al.*, 1996) with the following exceptions: cells to be assayed were labeled with BCEF (Molecular Probes, Eugene, OR), and after washing the assays, adhesion was quantitated by reading fluorescence in a Cytoflour plate reader (Perseptive Biosystems, Framingham, MA). Each condition in the assay was performed in triplicate. Assays were also normalized to the percent of transfected cells by FACS Adhesion assays are then reported with standard deviation and normalization factored into each condition.

For adhesion assays with soluble huMAdIg receptors, proteins were plated onto wells of a 96-well RIA plate (Costar, Cambridge, MA) at 0.2 µg/ml in 50 µl phosphate buffered saline (PBS). Plates were incubated overnight at 4°C, and blocked for 2 h at 37°C (PBS, 10% calf serum, Gibco). Labeled RPMI 8866 cells were added to each well at 1.25×10^6/well, then plates were incubated for 30 min at room temperature. Plates were for 2 cycles on a Microplate Autowasher (Biotek Instruments, Winooski, VT), then fluorescence quantitated. Each sample was assayed in triplicate and all assays were performed at least three times.

Purification of Mutant Ig-chimeras

Soluble chimeric proteins were produced by transient transfection of CHO/P cells as described above with the following exception: transfection media was replaced with 10 ml of MEM-α media approximately 18 h after transfection then incubated for 72–96 h at which time supernatants

were collected for purification. Chromatography columns (BioRad, Hercules, CA) were packed with 3 ml of Protein A Sepharose Fast Flow resin (Pharmacia Biotech, Uppsala, Sweden) and pre-equilibrated with PBS. Mutant Ig chimera supernatants were diluted 1:1 in PBS, filtered and applied to columns by gravity flow. Columns were washed with 60 ml PBS, then material eluted by addition of 4 ml of 0.1 M citrate pH 3.5, neutralized and dialyzed against PBS.

Soluble proteins were quantitated by ELISA. Ninety-six-well plates (NUNC Maxisorb, Boston, MA) were pre-coated with anti-human IgG (Jackson Immuno-Research, West Grove, PA), 10 μg/ml, 50 μl/well in carbonate buffer pH 9.5 and incubated overnight at 4°C, then blocked with PBS/5% gelatin for 2 h at 37°C. Samples and standard (human IgG1) were diluted in 1× THST (1 mM glycine, 0.5 M NaCl, 50 mM Trizma base pH 8.0, 0.05% Tween 20), applied to plates, and incubated for 2 h at room temp. Plates were rinsed with 1× THST. Detection was via peroxidase-conjugated goat-anti-mouse IgG (Jackson), 1:4000 in 1× THST, 50 μl/well. Assay was visualized with OPD (Sigma, Saint Louis, MO) and absorbance was read at 490 nm.

ELISA to Look at Structure of Mutated Receptors

NUNC (Boston, MA) 96-well plates were pre-coated with anti-human IgG (Jackson), 10 μg/ml, 50 μl/well in carbonate buffer pH 9.5, incubated overnight at 4°C, then blocked with PBS/10% FBS for 2 h 37°C. Plates were rinsed with 1× THST, then Ig chimera proteins were added to wells, 0.2 μg/ml, 50 μl/well in THST diluent, and incubated for 2 h at ambient temperature. Following a wash with THST, anti-huMAdCAM mAbs were added to wells (50 μl/well of hybridoma supernatants diluted 1:4 in THST), and plates were incubated 2 h at RT. Detection was via goat-anti-mouse IgG-HRP (Jackson), 1:2000 in THST, 50 μl/well, and assay was visualized with OPD reagent and absorbance was read at 490 nm.

RESULTS

Generation and Testing of Chimeric MAdCAM-1/VCAM-1 Receptors

MAdCAM-1 and VCAM-1 both bind $\alpha 4$ integrins, but differ in preferring $\alpha 4\beta 7$ versus $\alpha 4\beta 1$, respectively. To identify sequences in MAdCAM-1 that confer the preference in binding to $\alpha 4\beta 7$, we generated a series of chimeric MAdCAM-1/VCAM-1 receptors. We initially compared MAdCAM-1 to a construct of VCAM-1 that contained IgSF domains 1, 2, 3 and 7 (V1–3, 7) which contains a single VLA-4 binding site in domain 1 but lacks the second site in domain 4 (Osborn *et al.*, 1994; Vonderheide *et al.*, 1994). Transient expression of this construct in CHO/P cells resulted in avid binding of both RAMOS cells (which only express $\alpha 4\beta 1$) and RPMI 8866 cells (which exclusively express $\alpha 4\beta 7$) to levels largely indistinguishable from that of seven domain VCAM-1 (not shown) corroborating previous results that a single VLA-4 binding site was sufficient for interactions (Renz *et al.*, 1994; Vonderheide *et al.*, 1994). Adhesion assays performed with RPMI 8866 cells shows that levels of $\alpha 4\beta 7$ binding to MAdCAM-1 are similar at both ambient temperate and at 4°C but binding to V1–3,7 is abolished at 4°C (Fig. 1A). This difference in temperature dependence suggests that $\alpha 4\beta 7$ binding to MAdCAM-1 is a higher affinity interaction. Additionally, while the anti-human $\alpha 4\beta 7$ mAb ACT-1 completely inhibits binding to MAdCAM-1, it actually increased $\alpha 4\beta 7$ binding to VCAM-1, an observation consistent with previous published data (Schweighoffer *et al.*, 1993). These results suggest either structural differences in the $\alpha 4\beta 7$ binding site between these receptors, or a different orientation of the domains in MAdCAM-1 and V1–3,7 when bound to $\alpha 4\beta 7$.

A reciprocal exchange of domain 1 between native MAdCAM-1 and V1–3,7 was used to make the constructs M1,V2,3,7 and V1M2 (Fig. 1B). $\alpha 4\beta 7$ binding to these chimeras was examined in the RPMI 8866 cell binding assay (Fig. 1B). The chimeric protein V1M2 efficiently binds $\alpha 4\beta 7$ on RPMI 8866 cells and adhesion (in sharp contrast

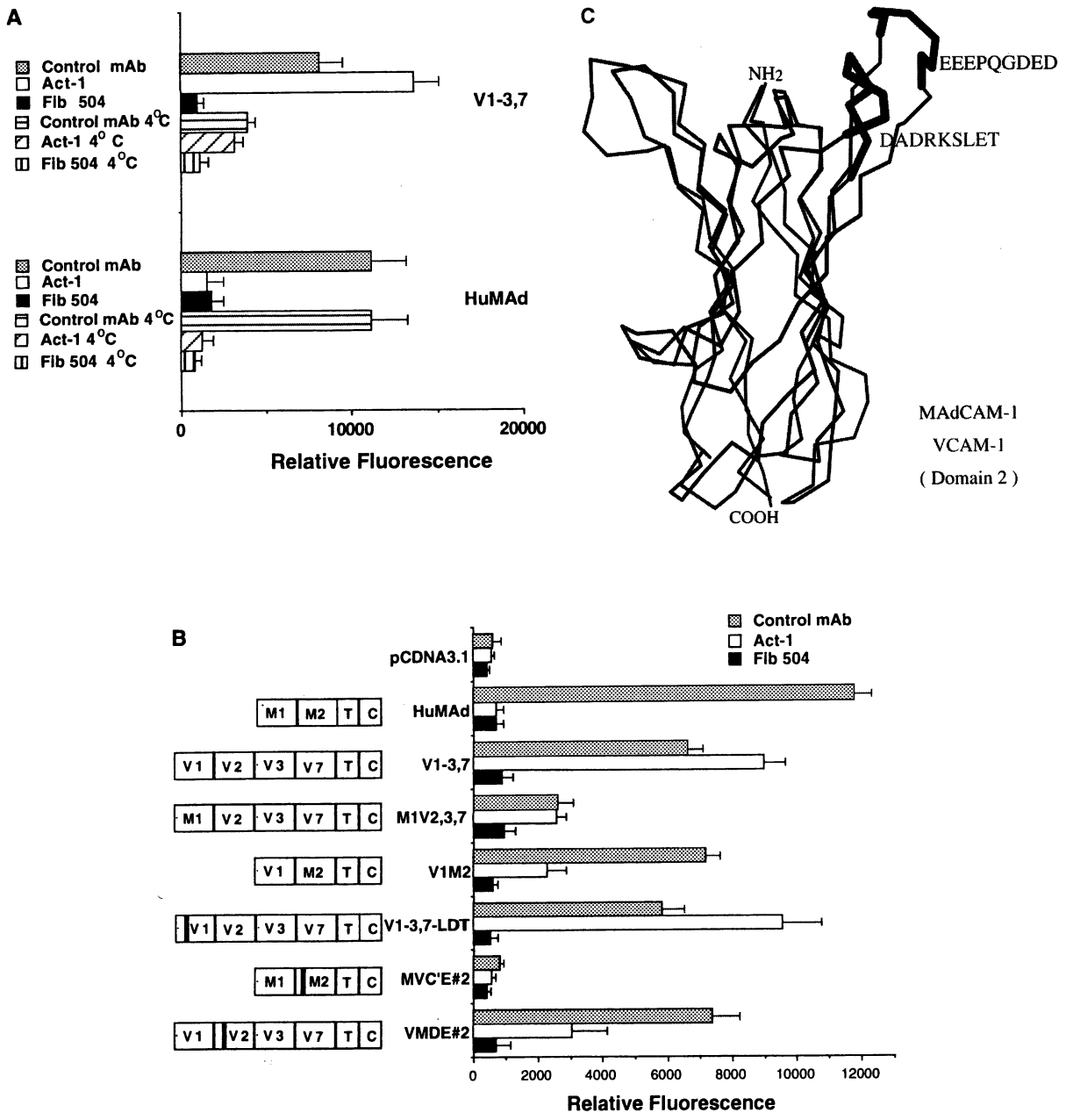

FIGURE 1 $\alpha4\beta7$ binding to MAdCAM-1 and VCAM-1 transfectants. (A), Adhesion of RPMI 8866 cells (which express high levels of $\alpha4\beta7$ and not $\alpha4\beta1$) to transiently transfected CHO/P cells expressing MAdCAM-1 or 4 domain (as described) VCAM-1 at 25°C and 4°C. Binding is shown as the average fluorescence of three wells with standard deviation. (B), Effects of domain and loops swaps on $\alpha4\beta7$ binding. Cartoons on the left illustrate the structure of each domain swap and loop swap, where the bold line approximates the location of the transposed loop. (C), Superposition of domain 2 between MAdCAM-1 (shown in blue) and VCAM-1 (shown in red). The charged residues of the C'E loop and DE loop of VCAM-1 and MAdCAM-1 that were exchanged in the chimeric receptor binding assay are highlighted. This figure was prepared with molscript (Kraulis, 1991). (See Color Plate I.)

to V1–3,7) is largely inhibited by the ACT-1 while $\alpha4\beta7$ binding to M1,V2,3,7 is substantially diminished (Fig. 1B). Binding to both of these chimeras is $\beta7$ dependent as pre-treatment with the anti-$\beta7$ mAb Fib-504 reduced adhesion to background levels. Expression of both chimeras, assessed with mAbs to MAdCAM-1 was similar to native MAdCAM-1 (not shown) suggesting that alterations in binding are not due to differences in levels of chimera expression. Additionally, when we insert the MAdCAM-1 domain 1 CD loop motif GLDTS in the VCAM-1 backbone (in place of QIDSP) to make V1–3,7-LDT, we find no difference in binding and mAb inhibition from V1–3,7 (Fig. 1B). These data indicate that the second Ig domain of MAdCAM-1 greatly influences binding to $\alpha4\beta7$.

The second domains of VCAM-1 and MAdCAM-1 differ in the position of strands on one edge of the Ig domain and belong to different Ig domain subsets. Whereas domain 2 of VCAM-1 was previously considered in the C2 set, it is now recognized as an I2 set domain (21, 39). By contrast, domain 2 of MAdCAM-1 belongs to the I1 set. Thus on the unique edge of domain 2, VCAM-1 has a C′ strand and a C′E loop whereas MAdCAM-1 has instead a D strand and a DE loop (Fig. 1C) (20). The DE loop is longer than the C′E loop of VCAM, is predominated by negatively charged residues and has the structure of an extended β-ribbon. Superpositions of D2 of MAdCAM-1 and VCAM-1 (Fig. 1C) highlights the C′E and DE loops and the key charged residues. We swapped these two motifs between MAdCAM-1 and VCAM-1 to examine their influence on binding. Both chimeric proteins, termed MVC′E#2 and VMDE#2 were expressed at high levels similar to native MAdCAM-1 and VCAM-1 (not shown). Adhesion assays with RPMI 8866 cells illustrate similar levels of binding when comparing V1–3,7 with VMDE#2 (Fig. 1B). Although levels of adhesion are quite similar, this region is suggested to have an influence on the $\alpha4\beta7$ binding interface as ACT-1 now significantly decreases binding to VMDE#2, much in the same manner as seen in the V1M2 chimeric protein (Fig. 1B). Conversely, expression of the VCAM-1 C′E region in MAdCAM-1 (MVC′E#2), resulted in greatly diminished $\alpha4\beta7$ binding. These data indicate that the DE β-ribbon in domain 2 of MAdCAM-1 is a critical component of the $\alpha4\beta7$ binding site.

Mutagenesis of Individual MAdCAM-1 Residues

In order to further define the $\alpha4\beta7$ binding site in MAdCAM-1 we generated a series of single amino acid substitutions in regions that, based upon other studies were predicted to be important for IgCAM/integrin interactions. We focused this study on selected interstrand loops in both domains 1 and 2 that were originally based upon the crystal structure of VCAM-1 and recently shown in the crystal structure of human MAdCAM-1 (Jones *et al.*, 1995; Tan *et al.*, 1998; Wang and Springer, 1998). The locations that were targeted are similar to interchain loops of other IgCAMs that have been shown to be important in integrin recognition, namely the CD and EF loops of domain 1 and the DE and FG loops of domain 2 (Casasnovas *et al.*, 1997; 1998; Holness *et al.*, 1995; Jones *et al.*, 1995; Klickstein *et al.*, 1996; Newham *et al.*, 1997; Osborn *et al.*, 1994; Renz *et al.*, 1994; Staunton *et al.*, 1990; Viney *et al.*, 1997; Vonderheide *et al.*, 1994; Wang *et al.*, 1995). In most instances, alanine substitution was used, and included most amino acids in each region with the exception of small, hydrophobic resides (Fig. 2). All mutations were made on a soluble Ig-fusion protein consisting of the entire extracellular domain of human MAdCAM-1 fused to the entire constant region of an Fc mutated human IgG1 heavy chain (Tidswell *et al.*, 1997). Recombinant proteins were transiently produced in CHO/P cells, purified by Protein A Chromatography, and quantitated in an IgG based ELISA to ensure that similar amounts of receptors were used in each experiment.

Adhesion was compared to binding to the parental MAdCAM-1-Ig chimera in an RPMI 8866 cell binding assay, initially in the absence of activating stimuli. Alanine substitution of R39, L41, D42, T43, R70, E148, E151, E152, E157 and

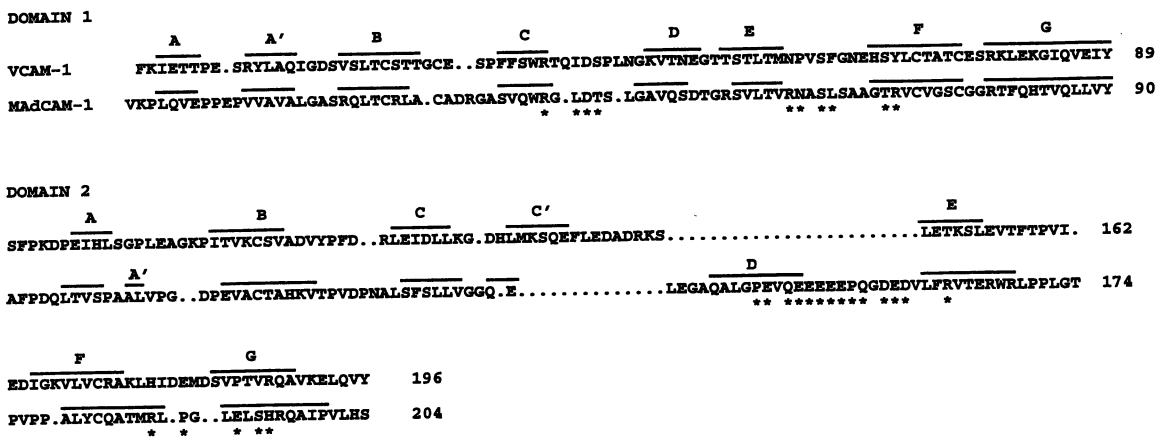

FIGURE 2 Structure based sequence alignment of MAdCAM-1 and VCAM-1. β-strands defined by DSSP (Kabsch and Sander 1983) are overlined. MAdCAM-1 residues that were chosen for mutagenesis are highlighted by an asterisk.

H195 all resulted in severe effects (judged by $< 25\%$ adhesion to wild type) of binding when compared to wild-type MAdCAM-1 (Table I). Additionally, a conservative change of D42E also resulted in no binding as adhesion was reduced to only 4.3% of normal. Moderate effects (25–50% adhesion) on binding were observed with S55A and E149A while mild effects (50–75% adhesion) were seen with L64A, Q147A and D156A. All other mutations did not result in significant changes in binding with the exception of R60A and E192A, which resulted in significant increases in binding (Table I).

To further assess the severity of the mutations tested, the assays were repeated in the presence of 1 mM Mn^{++}, which has been shown to fully activate integrins, including $\alpha 4\beta 7$ (Berlin *et al.*, 1993; Briskin *et al.*, 1996). Under these conditions, only three residues, L41A, D42A and E148A remained at less than 25% of adhesion of wild-type MAdCAM-1. Three other residues, R70A, E152A and E157A were still significantly affected in the presence of Mn^{++}. Additionally, the two mutations (R60 and E192) that showed increased binding were now binding at similar levels to the wild type MAdCAM-1 chimera (Table I).

The results of performing the assays with activated integrin were similar to looking at adhesion of the mutant receptors at a range of concentrations up to four fold higher than those used in the previous adhesion assays. The severe mutations such as L41A and D42A could not be rescued by using higher receptor densities while binding to R39A and T43a were largely restored when binding to higher receptor densities (Fig. 3A). The R70A mutation was similar to the L41 and D42 mutations as it could not be rescued at higher densities while binding to L64 was mostly restored at higher concentrations (Fig. 3B). The mutations that were examined in the DE β-ribbon of domain 2 were restored to levels closer to native MAdCAM (similar to binding to Mn^{++} treated cells) at higher receptor densities, including E148A, E149A, D156A and E157A. The E157 mutation was the most severe in this analysis (Fig. 3C). These data suggest the mutations in the β-ribbon might have different mechanistic effects on binding than the CD loop mutations in domain 1.

Structural Analysis with Domain Specific Antibodies

A panel of anti-human MAdCAM-1 mAbs were previously raised against murine pre-B cells (L1-2) stably transfected with human MAdCAM-1 cDNA (Briskin *et al.*, 1997). These antibodies were mapped to Ig domains 1 or 2 by flow cytometric analysis of

TABLE I Summary of analysis of MAdCAM-1 point mutations

Mutant	Without Mn^{++}		With Mn^{++}		Domain one			Domain two							Anti-hIgG
	Mean	SD	Mean	SD	5E10	7H12	10G3	8C1	10A6	3B11	9G12	1E10	1E5	4G5	
R39A	20.48	8.24	62.25	3.14	98	84	89	89	88	83	87	85	86	80	73.9
L41A	0.25	0.50	10.88	3.39	95	95	100	100	97	82	98	96	96	94	96.6
D42A	1.38	2.75	1.5	1.24	93	96	96	97	102	110	97	96	93	98	93.4
D42E	4.3	8.53	23.1	5.08	97	93	98	98	98	125	98	94	93	98	100
D42E	4.3	8.53	23.1	5.08	97	93	98	98	98	125	98	94	93	98	100
T43A	5.08	4.44	54.5	3.56	98	93	96	92	93	117	91	89	92	90	83.9
S55A	27.94	25.21	88.65	5.17	95	97	77	95	95	103	92	96	93	100	92.3
R60A	224.68	27.10	97.4	5.89	88	100	93	89	94	103	84	96	96	97	95.4
N61A	118.23	38.56	88.2	6.23	96	92	93	94	94	84	83	94	91	92	96.3
L64A	59.8	19.11	81.9	3.20	94	102	98	93	96	85	93	100	95	96	70
S65A	101.2	31.20	84.4	4.30	91	98	99	94	94	101	92	97	95	97	89
T69A	144.73	38.07	83.93	7.25	92	92	93	97	92	59	93	91	85	78	85.6
R70A	1.05	1.22	48.4	4.3	93	85	92	89	86	41	80	86	83	67	113.5
Q147A	73.8	14.00	71.5	6.8	100	96	96	9	75	63	7	93	9	86	75
E148A	1.43	1.67	22.6	5.05	81	69	78	61	62	40	62	63	61	41	95.6
E149A	37.9	23.80	62.9	9.20	99	72	71	69	83	74	66	82	66	59	63
E150A	116.85	23.05	82.58	2.22	97	94	91	94	95	140	91	94	93	94	83.9
E151A	6.18	7.15	67.3	0.42	87	59	61	56	64	49	55	59	57	46	100
E152A	0.8	0.98	29.2	6.08	95	84	89	84	84	72	71	77	72	68	102.1
Q154A	91.04	34.00	72.1	9.10	91	74	77	77	75	120	72	76	72	71	86.4
D156A	56.08	6.78	65.78	13.65	96	89	92	43	7.4	111	7.2	90	98	87	73.8
E157A	8.6	5.27	49.15	12.20	96	92	93	94	94	84	83	94	91	92	111.2
E192A	147.95	4.14	85.65	3.80	94	84	84	86	88	90	83	86	85	80	100
H195A	22.45	10.31	66.78	6.88	93	106	101	100	107	87	96	104	103	108	88
R196A	86.03	15.91	71.43	4.57	98	93	94	96	97	111	94	94	96	98	91.7
VCAMIg	N/A	N/A	N/A	N/A	11.9	19.4	6.5	7.5	7.1	10.5	7.4	17.1	7.9	7	112

Listed are all mutations which resulted in significant effects on adhesion and some mutants with minimal effects such as N61, T69, Q147, E150 and R196. Percent adhesion relative to wild-type MAdCAM-1-Ig chimera (defined as 100%) in the absence and presence of Mn^{++} stimulation is listed. Also shown for each mutant are the results of an ELISA with anti-MAdCAM-1 mAbs that map to domain one or domain two as indicated, along with anti-human IgG to show that similar amounts of protein are used. Results indicate percent of mAb binding to MAdCAM-1 Ig as control. Soluble VCAM-1-Ig chimera is used as a negative control for mAb binding.

CHO/P cells transiently transfected with native MAdCAM-1 or the V1M2 and M1,V2,3,7 chimeras (not shown). Competitive inhibition assays (data not shown) were used to select mAbs that each recognized distinct regions of MAdCAM-1 in both Ig domains 1 and 2.

All of the mAbs utilized efficiently bound the mutations in domain 1 (defined as > 70% of binding to native MAdCAM-1) indicating that the overall conformation and orientation of both domain 1 and 2 was retained (Table I). This observation is consistent with analysis of similar regions in other CAMs which indicate that the CD loop, being surface exposed, is not involved in maintenance of overall structure (Holness *et al.*, 1995; Newham *et al.*, 1997; Osborn *et al.*, 1994; Renz *et al.*, 1994; Viney *et al.*, 1997). The only exception in domain 1 was reduced binding of mAb 3B11 to both T69A and R70A, which lie outside of the CD loop. Interestingly, while these residues are located in domain 1, the 3B11 mAb maps to domain 2. In domain 2, several of the mutations including Q147A, E148A, E149A, E151A, and D156A resulted in reduction of binding of several mAbs, including, in some instances (E151) effects in D1 specific epitopes as well as D2.

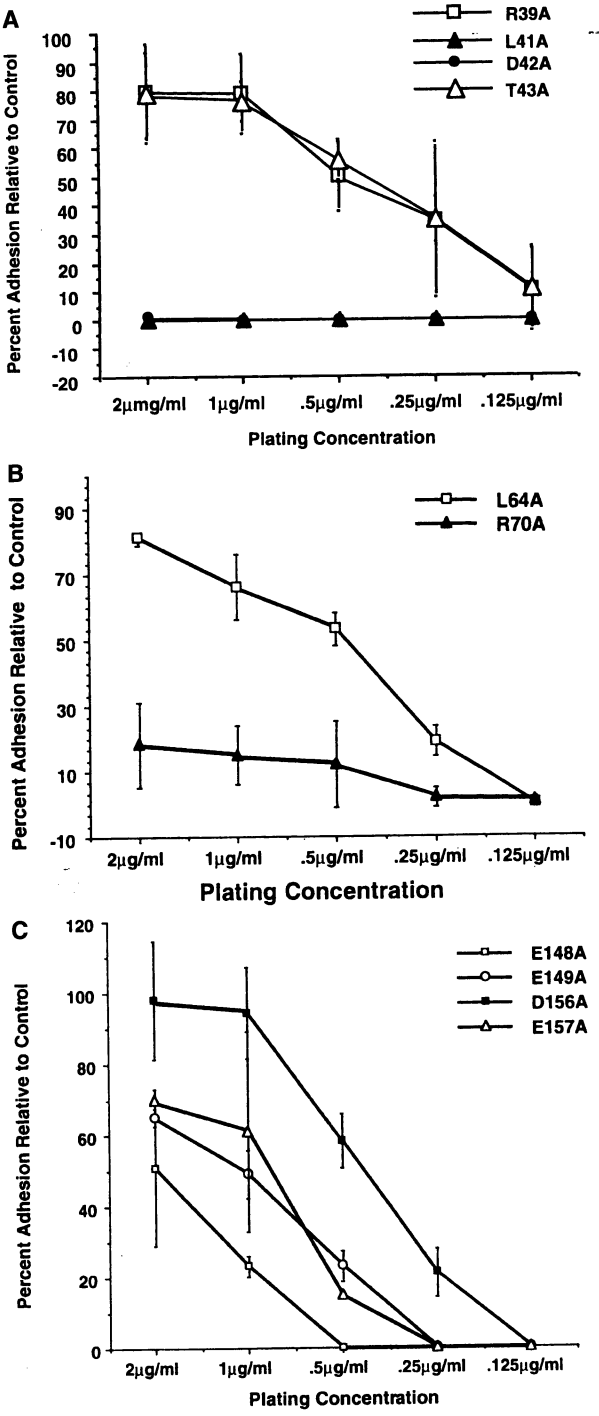

FIGURE 3 Concentration curves of representative mutations. (A), Binding to significant residues in the CD loop. (B), Binding to L64 in the EF loop and the internally located R70A mutation. (C), Binding to selected acidic residues in the DE β-ribbon.

DISCUSSION

Structure/function studies with vascular Ig-like adhesion receptors have shown that the two N-terminal Ig domains of all IgCAMs are sufficient for efficient binding to their respective integrin ligands (Briskin *et al.*, 1996; Holness *et al.*, 1995; Osborn *et al.*, 1992; Pepinsky *et al.*, 1992; Renz *et al.*, 1994; Staunton *et al.*, 1990). Within the first Ig-like domain, all IgCAMs additionally share the feature of a conserved sequence, G-(I/L)-(D/E)-(T/S)-(P/S)-L in the region of β-strands C and D; mutagenesis of the central aspartate/glutamate residue completely abrogates integrin binding (Holness *et al.*, 1995; Klickstein *et al.*, 1996; Newham *et al.*, 1997; Osborn *et al.*, 1994; Renz *et al.*, 1994; Staunton *et al.*, 1990; Viney *et al.*, 1997; Vonderheide *et al.*, 1994). The conservation of this motif, along with experiments where CD loops have been swapped without changing integrin binding preference (Newham *et al.*, 1997; Osborn *et al.*, 1994), suggests that other elements are also required for integrin binding specificity. Domain swap experiments with the α4 ligands VCAM-1 and MAdCAM-1 also show that the amino terminal Ig-domain fails to bind efficiently when fused to other Ig regions, suggesting that the regions for specific and efficient binding must extend into domain two (Briskin *et al.*, 1996; Osborn *et al.*, 1992; Pepinsky *et al.*, 1992). This might be a feature unique to IgCAMs which bind to α4 integrins as studies with ICAM-3 have shown that domain 1 is sufficient to efficiently bind LFA-1 (Klickstein *et al.*, 1996).

In this study we show, by use of chimeric VCAM/MAdCAM receptors and site directed mutagenesis, that the region of human MAdCAM-1 necessary for $\alpha4\beta7$ binding requires conserved residues in the CD loop, but additionally utilizes unique residues that extend over a region encompassing both Ig domains 1 and 2. A chimeric protein, consisting of VCAM-1 domain 1 fused to domain 2 of MAdCAM-1 (V1M2) binds $\alpha4\beta7$ more efficiently than a chimera containing domain 1 of MAdCAM-1 fused to domains 2, 3 and 7 (M1,V2,3,7) of VCAM-1. The anti-$\alpha4\beta7$ mAb Act-1 inhibits (as it does in $\alpha4\beta7$

binding to MAdCAM-1) binding to V1M2 while it augments $\alpha4\beta7$ adhesion to native VCAM-1. These data extend previous observations about differences in the effects of this blocking mAb (Erle *et al.*, 1994; Shyjan *et al.*, 1996) by illustrating that domain 2 of MAdCAM-1 largely contributes to the $\alpha4\beta7$ binding site.

The most unique feature in domain 2 of MAdCAM-1 is the highly extended DE β-ribbon-like structure (Figs. 1C and 4). While the $\alpha4$ integrin ligands VCAM-1 and MAdCAM-1 both contain an extended loop in domain 2 (which is a C′E loop in VCAM-1), superposition of domain 2 in these receptors shows that the orientation of these loops are quite different (Fig. 1C). Insertion of the DE loop into VCAM resulted in a chimeric receptor that functioned identically to V1M2 (Fig. 1B), illustrating that this motif significantly affects binding to $\alpha4\beta7$.

We proceeded to perform site directed mutagenesis to further define critical ($\alpha4\beta7$ binding residues in both Ig domains one and two. Our results confirm data on other IgCAMs that an essential contact site resides in the CD loop in domain one, the most significant residues being L41 and D42 (Table I). Alanine substitution in either of these sites abolishes integrin interactions, even when $\alpha4\beta7$ is fully activated by Mn^{++} or when examining binding to higher densities of these mutated proteins (Table I, Fig. 3A) Additionally, a conservative substitution, D42E, also resulted in complete abrogation of binding. A homologous mutation in VCAM-1, D40E (Newham *et al.*, 1997) completely abolishes binding to $\alpha4\beta7$ and markedly reduces adhesion to $\alpha4\beta1$. Similarly, the CD loop peptide LDTSL can inhibit $\alpha4\beta7$ binding to MAdCAM-1 (Shroff *et al.*, 1996) while the closely related peptide LETSL is inactive (Shroff and Briskin, unpublished data). Residues L41 and D42 in MAdCAM-1 are oriented on the tip of the protruding CD loop in a position analogous to that in VCAM-1 (Fig. 4) (Jones *et al.*, 1995; Tan *et al.*, 1998; Wang and Springer, 1998); this loop is unique to IgCAMs that bind $\alpha4$ integrins. While this feature might partially explain the ability of these receptors to mediate primary (rolling) interactions with their counter-ligands, it fails to explain integrin binding preference. When we insert the CD loop of MAdCAM-1 into VCAM-1 we see no differences in $\alpha4\beta7$ binding in comparison to VCAM-1 (Fig. 1B). Recently, a similar study showed that the CD loop of murine MAdCAM-1 swapped into VCAM-1 resulted in a receptor with a hyper-adhesive phenotype, but this was true for binding to both $\alpha4\beta7$ and $\alpha4\beta1$ (Newham *et al.*, 1997). While our results differ in failing to observe an increase in adhesion (likely due to subtle differences in assays), in neither case was the integrin binding specificity changed, further reinforcing the notion that the specificity on the integrin binding site extends to regions beyond the CD loop.

Another region we focused is the interconnecting loop and the E and F strands in domain one. Within this region, critical residues for integrin binding have been observed in many IgCAMs including VCAM-1, ICAM-1 and ICAM-3 (Holness *et al.*, 1995; Klickstein *et al.*, 1996; Newham *et al.*, 1997; Osborn *et al.*, 1994; Staunton *et al.*, 1990) as well as domain 3 of ICAM-1, where mutation of the EF loops affected binding to Mac-1 (Diamond *et al.*, 1991). The most dramatic effect of mutagenesis in this region of MAdCAM-1, R70A, maps to the F strand and is buried in a core of hydrophobic residues (Fig. 4). Mutation of this residue results in complete loss of binding and, similar to D41A and L42A, also binds poorly to Mn^{++} activated $\alpha4\beta7$ and higher MAdCAM-1 plating densities (Table I, Fig. 3B). The guanadinium group of R70 hydrogen bonds to the mainchain atoms of three residues, A66 in the F strand and L42 and T 43 in the CD loop, suggesting that this residue plays a critical role by maintaining a rigid conformation of the CD and EF loops (Tan *et al.*, 1998; Wang and Springer, 1998). Along these lines, we and others have demonstrated the requirements for a constrained configuration by showing that CD loop based linear peptides of both VCAM-1 and MAdCAM-1 are less potent then their cyclized derivatives (Shroff and Briskin, unpublished data.) (Wang *et al.*, 1995).

The other significant mutations in domain 1 of MAdCAM-1 are S55A and L64A. S55A is buried in

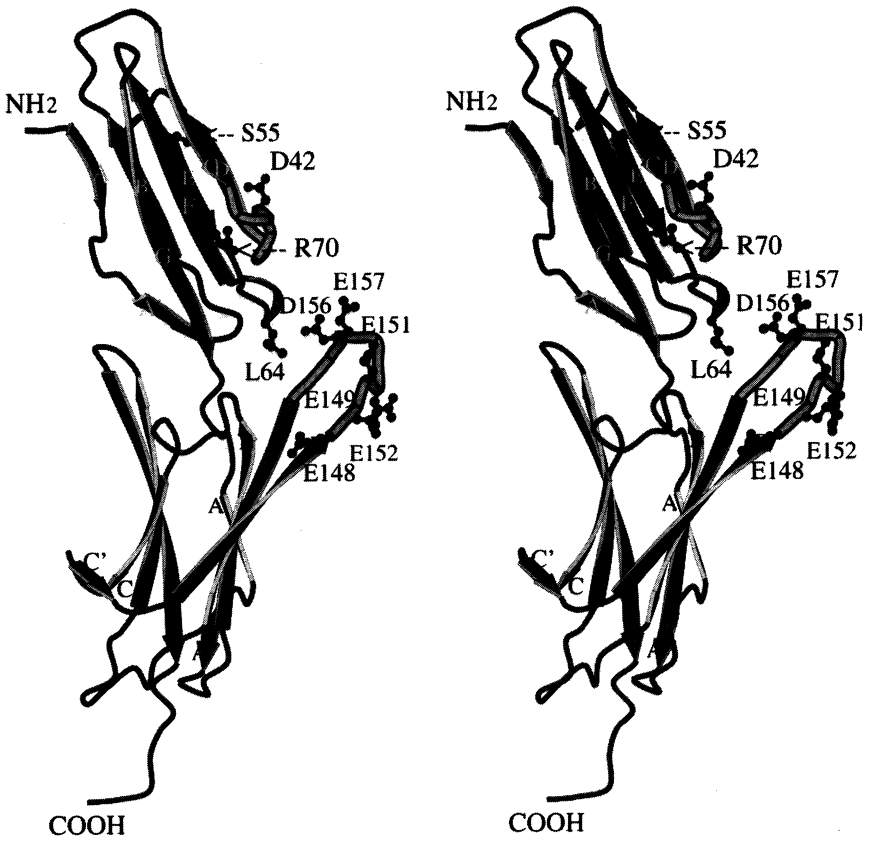

FIGURE 4 Stereoview of the crystal structure of MAdCAM-1. Domain 1 is highlighted in red and domain 2 in green. The CD loop and the DE β-ribbon of domains 1 and 2 respectively are highlighted in yellow and the EF loop in domain 1 in blue. Key residues that effect adhesion are shown as ball and stick. All mutations shown resulted in reduced adhesion to $\alpha 4\beta 7$. This figure was prepared with molscript (Kraulis, 1991). (See Color Plate II.)

the core of D1 and forms a hydrogen bond with W38, thus providing structural stability, whereby mutagenesis might modify the conformation of the CD loop binding motif. This mutant illustrates a similar structural feature, since a similar side chain hydrogen bond is also found in other Ig family members such as CD2, CD4 and VCAM-1. L64A maps to the EF loop and is the beginning of a short α-helix. The side chain of L64 points downward and may interact with the DE β-ribbon of D2, and the mutation may destabilize that loop (Fig. 4). Individual mutations (see below) in the DE β-ribbon have severe effects on binding and may be complementary to L64. Interestingly, E66 in the GNEH motif of VCAM, when mutagenized has marked effects on binding $\alpha 4\beta 7$, with little effect on $\alpha 4\beta 1$ binding (Chiu *et al.*, 1995; Kilger *et al.*, 1997). This residue, also in the EF loop points toward domain 2 and might, in similar fashion to L64 interact with the C'E loop of VCAM-1.

Mutational analysis within domain 2 of MAdCAM-1 reinforces the significance of the DE ribbon in adhesion to $\alpha 4\beta 7$. Alanine substitution of 6 of the 9 acidic residues in this loop resulted in significant loss of binding (Table I). Mutation of E148A resulted in severe reduction of adhesion along with reduced binding of all D2 specific mAbs. E148 lies at the end of the D strand its mutation might affect

the orientation of DE loop. However, mutation of several acidic amino acids within the DE loop that have no obvious structural role results in both reduction in cell adhesion and binding of many mAbs and in some instances, reduction in binding domain 1 specific epitopes as well (Table I). Mutation of one residue in particular, E151A, resulted in significant loss of mAb binding with all mAbs except one (Table I), while similar (but less severe) effects were seen for E149A and E152A. The effects of these mutations might be to change the electrostatic character of the β-ribbon, which might in turn affect the general orientation of domain 1 with respect to domain 2. The reduction in antibody binding observed might be interpreted as a change in accessibility of mAb binding sites, as opposed to a general perturbation of domain structure.

Several of the functionally important residues in the DE loop might serve as additional integrin contact sites, especially D156 and E157, as their orientation lies in the direction of the CD and EF loops in domain 1. E157 is the closest exposed residue in the DE loop to D42, with a distance of approximately 20 Å and this residue (as well as D156), might coordinate interactions with one integrin chain while the residues of the CD loop interact with the other chain. Alternatively, the loop might electrostatically guide integrin contact with the CFG face of domain one, thereby increasing the on rate for binding. The DE loop may also be analogous to the synergy sequence that has been described in fibronectin. The X-ray structure for the RGD binding region of fibronectin reveals an anti-parallel array of β-strands similar to an Ig domain. While the RGD motif is located in the 10th type III repeat, peptide inhibition studies have shown the existence of a second binding site, termed the synergy site which also resides in a C′E loop and part of the E strand (Aota *et al.*, 1994; Leahy *et al.*, 1996). The distance between the synergy sites and RGD (approximately 30–40 Å) is similar to the distance between the DE loop and the CD loop of MAdCAM-1 and a similar relationship also exists between the C′E and CD loops of VCAM-1. In all of these examples, these regions are exposed on the same face of adjacent domains (Fig. 4). In accordance with our observations, mutations in several residues in the C′E loop of VCAM-1 had significant effects on adhesion to both $\alpha4\beta1$ and $\alpha4\beta7$ (Newham *et al.*, 1997). Interestingly, the mutations in the C′E region of VCAM-1 had a greater effect on adhesion to $\alpha4\beta7$ binding than to $\alpha4\beta1$. The majority of severe mutations in this study were also acidic residues, reinforcing the importance of negatively charged amino acids in this region in conferring $\alpha4\beta7$ binding. Furthermore the mutations, while overlapping were not identical in their effects on binding these two integrins, further suggesting that the loop might play an important role in defining integrin binding specificity.

In summary, we have demonstrated that the residues critical for $\alpha4\beta7$ binding to MAdCAM-1 map to the same face of the receptor and extend across both domains one and two. These unique regions for binding map to novel sites in this receptor that are readily interpreted in the structure of human MAdCAM-1 These studies suggest that the preference for integrin binding is likely to result from a combination of multiple binding and structural motifs, which include the CD loop, a buried arginine (R70) residue in domain 1 and elements of the EF loop and the large β-ribbon in domain 2. In addition to the insights gained in understanding $\alpha4\beta7$ binding to MAdCAM-1,these observations should aid in our understating of integrin–IgCAM interactions as a whole and in the design on specific anti-adhesive drugs.

Acknowledgments

We would like to thank Walter Newman for critical reading of this manuscript.

References

Andrew, D.P., Berlin, C., Honda, S., Yoshimo, T., Hamann, A. *et al.* (1994) Distinct but overlapping epitopes are involved in $\alpha_4\beta_7$-mediated adhesion to vascular cell adhesion molecule-1, mucosal addressin-1, fibronectin, and lymphocyte aggregation. *J. Immunol.* **153**, 3847–3861.

Aota, S.-I., Nomizu, M. and Yamada, K.M. (1994) The short amino acid sequence PROHIS-SER-ARG-ASN in human fibronectin enhances cell-adhesive function. *J. Biol. Chem.* **269**, 24756–24761.

Berlin, C., Berg, E.L., Briskin, M.J., Andrew, D.P., Kilshaw, P.J. *et al.* (1993) $\alpha4\beta7$ integrin mediates lymphocyte binding to the mucosal vascular addressin MAdCAM-1. *Cell* **74**, 185–195.

Briskin, M.J., McEvoy, L.M. and Butcher, E.C. (1993) MAdCAM-1 has homology to immunoglobulin and mucin-like adhesion receptors and to IgA1. *Nature* **363**, 461–464.

Briskin, M.J., Rott, L.S. and Butcher, E.C. (1996) Structural requirements for mucosal vascular addressin binding to its lymphocyte receptor $\alpha4\beta7$: Common themes among integrin-Ig family interactions. *J. Immunol.* **156**, 719–726.

Briskin, M.J., Winsor-Hines, D., Shyjan, A.M., Cochran, N., Bloom, S. *et al.* (1997) Human mucosal addressin cell adhesion molecule-1 (MAdCAM-1) is preferentially expressed in intestinal tract and associated lymphoid tissues. *Am. J. Path.* **151**, 97–109.

Butcher, E.C. (1991) Leukocyte-endothelial cell recognition: three (or more) steps to specificity and diversity. *Cell* **67**, 1033–1036.

Casasnovas, J.M., Springer, T.M., Liu, J.-H., Harrison, S.C. and Wang, J.-H. (1997) Crystal structure of ICAM-2 reveals a distinctive integrin recognition surface. *Nature* **387**, 312–315.

Casasnovas, J.M., Stehle, T., Liu, J.-H., Wang, J.-H. and Springer, T.M. (1998) A dimeric crystal structure for the N-terminal two domains of intercellular adhesion molecule-1. *Proc. Natl. Acad. Sci. USA* **95**, 4134–4139.

Chiu, H.H., Crowe, D.T., Renz, M.E., Presta, L.G., Jones, S. *et al.* (1995) Similar but non identical amino acid residues on vascular cell adhesion molecule-1 are involved in the interaction with alpha 4 beta 1 and alpha 4 beta 7 under different activity states. *J. Immunol.* **155**, 5257–5267.

Diamond, M.S., Staunton, D.E., Marlin, S.D. and Springer, T.A. (1991) Binding of the integrin MAC-1 (CD11b/CD18) to the third immunoglobulin-like domain of ICAM-1 (CD54) and its regulation by glycosylation. *Cell* **65**, 961–971.

Erle, D.J., Briskin, M.J., Butcher, E.C., Garcia-Pardo, A., Lazarovits, A.I. and Tidswell, M. (1994) Expression and function of the MAdCAM-1 receptor, integrin $\alpha4\beta7$, on human leukocytes. *J. Immunol.* **153**, 517–528.

Graber, N., Venkat Gopal, T., Wilson, D., Beall, L.D., Polte, T. and Newman, W. (1990) T cells bind to cytokine-activated endothelial cells via a novel, inducible sialoglycoprotein and endothelial leukocyte adhesion molecule-1. *J. Immunol.* **145**, 819–830.

Heffernan, M. and Dennis, J.D. (1991) Polyoma and hamster papovavirus large T antigen-mediated replication of expression shuttle vectors in Chinese hamster ovary cells. *Nucl. Acids Res.* **19**, 85.

Hesterberg, P.E., Windsor-Hines, D., Briskin, M.J., Soler-Ferran, D., Merrill, C. *et al.* (1996) Rapid resolution of chronic colitis in the cotton-top tamarin with an antibody to a gut homing integrin $\alpha4\beta7$. *Gastroenterology* **111**, 1373–1380.

Holness, C.A., Bates, P.A., Littler, A.J., Buckley, C.D., McDowall, A.L. *et al.* (1995) Analysis of the binding site on intracellular adhesion molecule 3 for the leukocyte integrin lymphocyte function-associated antigen-1. *J. Biol. Chem.* **270**, 877.

Jones, E.Y., Harlos, K., Bottomley, M.J., Robinson, R.C., Driscoll, P.C. *et al.* (1995) Crystal structure of an integrin-binding fragment of vascular cell adhesion molecule-1 at 1.8 A resolution. *Nature* **373**, 539–544.

Kabsch, K. and Sander, C. (1983) Dictionary of protein secondary structure: pattern recognition of hydrogen-bonded and geometrical features. *Biopolymers* **22**, 2577–2637.

Kilger, G., Clements, J. and Holzman, B. (1997) Amino acid residues required for binding of vascular cell adhesion molecule-1 to integrin $\alpha4\beta7$. *International Immunology* **9**, 219–226.

Klickstein, L.B., York, M.R., de Fougerolles, A.R. and Springer, T.A. (1996) Localization of the binding site on intercellular adhesion molecule-3 (ICAM-3) for lymphocyte-function-associated antigen 1 (LFA-1). *J. Biol. Chem.* **271**, 23920–23927.

Kraulis, P. (1991) MOLSCRIPT: a program to produce both detailed and schematic plots of protein structure. *J. Appl. Crystallogr.* **24**, 946–950.

Lazarovits, A.I., Moscicki, R.A., Kurnick, J.T., Camerini, D., Bhan, A.K. *et al.* (1984) Lymphocyte activation antigens: I. amonoclonal antibody, anti-Act I, defines a new late lymphocyte activation antigen. *J. Immunol.* **133**, 1857.

Leahy, D.J., Aukhil, A. and Erickson, H.P. (1996) 2.0 A crystal structure of a four-domain of human fibronectin encompassing the RGD loop and synergy region. *Cell* **84**, 155–164.

Newham, P., Craig, S.E., Seddon, G.N., Schfield, N.R., Rees, A. *et al.* (1997) $\alpha4$ integrin binding interfaces on VCAM-1 and MAdCAM-1 integrin binding footprints identify accessory binding sites that play a role in integrin specificity. *J. Biol. Chem.* **272**, 19429–19440.

Osborn, L., Vassallo, C. and Benjamin, C.D. (1992) Activated endothelium binds lymphocytes through a novel binding site in the alternately spliced domain of vascular cell adhesion molecule-1. *J. Exp. Med.* **176**, 99–107.

Osborn, L., Vassallo, C., Browning, B.G., Tizard, R., Haskard, D.O. *et al.* (1994) Arrangement of domains, and amino acid residues required for binding of vascular cell adhesion molecule-1 to its counter-receptor VLA-4 ($\alpha4\beta1$). *J. Cell Biol.* **124**, 601.

Pepinsky, B.C., Hession, L.-L., Chen, P., Moy, L., Burky, A. *et al.* (1992) Structure/function studies on vascular cell adhesion molecule-1. *J. Biol Chem.* **267**, 17820–17826.

Picarella, D., Huribut, P., Rottman, J.R., Shi, X., Butcher, E. and Ringler, D.J. (1997) Monoclonal antibodies specific for $\beta7$ integrin and mucosal addressin cell adhesion molecule-1 (MAdCAM-1) reduce inflammation in the colon of scid mice reconstituted with CD45RB^{high} T cells. *J. Immunol.* **158**, 2099–2106.

Picker, L.J. and Butcher, E.C. (1992) Physiological and molecular mechanisms of lymphocyte homing. *Ann. Rev. Immunol.* **10**, 561–91.

Polte, T., Newman, W. and Venkat Gopal, T. (1990) Full-length vascular cell adhesion molecule-1. *Nucleic Acids Res.* **18**, 5901.

Renz, M.E., Chiu, H.H., Jones, S., Fox, J., Kim, K.J. *et al.* (1994) Structural requirements for adhesion of soluble recombinant murine vascular cell adhesion molecule-1 to $\alpha4\beta1$. *J. Cell Biol.* **125**, 1395–1406.

Rott, L.S., Briskin, M.J., Andrew, D.P., Berg, E.L. and Butcher, E.C. (1996) A fundamental subdivision of circulating lymphocytes defined by adhesion to mucosal addressin cell adhesion molecule-1. *J. Immunol.* **156**, 3727–3736.

Ruegg, C., Postigo, A.A., Sikorski, E.E., Butcher, E.C., Pytela, R. and Erle, D.J. (1992) Role of integrin $\alpha4\beta7/\alpha4\beta$P in lymphocyte adherence to fibronectin and VCAM-1 and in homotypic cell clustering. *J. Cell Biol.* **117**, 179–189.

Ruoslahti, E. (1991) Integrins. *J. Clin. Invest.* **87**(1), 1–5.

Schweighoffer, T., Tanaka, Y., Tidswell, M., Erle, D.J., Horgan, K.J. *et al.* (1993) Selective expression of integrin $\alpha_4\beta_7$ on a subset of human CD4M+ memory T cells with hallmarks of gut-trophism. *J. Immunol.* **151**, 717–729.

Shroff, H.N., Schwender, C.F., Dottavio, D., Yang, L.-L. and Briskin, M.J. (1996) Small peptide inhibitors of $\alpha4\beta7$-mediated MAdCAM-1 adhesion to lymphocytes. *Bioorg. Med. Chem.* **6**, 2495–2500.

Shyjan, A.M., Bertognolli, M., Kenney, C.J. and Briskin, M.J. (1996) Molecular cloning of human Mucosal Cell Adhesion Molecule-1 (MAdCAM-1) demonstrates structural and functional similarities to the $\alpha4\beta7$ integrin binding domains of murine MAdCAM-1 but extreme divergence of mucin-like sequences. *J. Immunol.* **156**, 2851–2857.

Springer, T.A. (1994) Traffic signals for lymphocyte recirculation and leukocyte emigration: the multistep paradigm. *Cell* **76**, 301–314.

Staunton, D.E., Dustin, M.L., Erickson, H.P. and Springer, T.A. (1990) The arrangement of the immunoglobulin-like domains of ICAM-1 and the binding sites for LFA-1 and rhinovirus. *Cell* **61**, 243.

Streeter, P.R., Lakey-Berg, E., Rouse, B.T.N., Bargatze, R.F. and Butcher, E.C. (1988) A tissue-specific endothelial cell molecule involved in lymphocyte homing. *Nature* **331**, 41–46.

Tan, K., Casasnovas, J.M., Liu, J.-H., Briskin, M.B., Springer, T.A. and Wang, J.-H. (1998) The strucutre of MAdCAM-1 reveals a "W" shaped motif in domain 1 and a novel DE ribbon in domain 2 involved in $\alpha4\beta7$ integrin binding. *Structure* **6**, 793–801.

Tidswell, M., Pachynski, R., Wu, S.W., Qiu, S.-Q., Dunham, E. *et al.* (1997) Structure/function analysis of the integrin $\beta7$ subunit: identification of domains involved in adhesion to MAdCAM-1. *J. Immunol.* **157**, 1497–1505.

Viney, J.L., Jones, S., Chiu, H.H., Lagrimas, B., Renz, M.E. *et al.* (1997) Mucosal addressin cell adhesion molecule-1: A structural and functional analysis demarcates the integrin binding motif. *J. Immunol.* **157**, 2488–2497.

Vonderheide, R.H., Tedder, T.F., Springer, T.A. and Stuanton, D. (1994) Residues within a conserved amino acid motif of domains 1 and 4 of VCAM-1 are required for binding to VLA-4. *J. Cell Biol.* **125**, 215.

Wang, J.-H., Pepinsky, R.B., Steele, T., Liu, J.-H., Karpusas, M. *et al.* (1995) The crystal structure of an N-terminal two-domain fragment of vascular cell adhesion molecule 1 (VCAM-1): A cyclic peptide based on the domain 1 C-D loop can inhibit VCAM-1-$\alpha4$ interaction. *Proc. Natl. Acad. Sci. USA* **92**, 5714–5718.

Wang, J.-h. and Springer, T.A. (1998) Structural specializations of immunoglobulin superfamily members for adhesion to integrins and viruses. *Immunological Reviews* **163**, 197–215.

Williams, M.B. and Butcher, E.C. (1997) Homing of naive and memory T lymphocyte subsets to peyer's patches, lymph nodes and spleen. *J. Immunol.* **159**, 1746–1752.

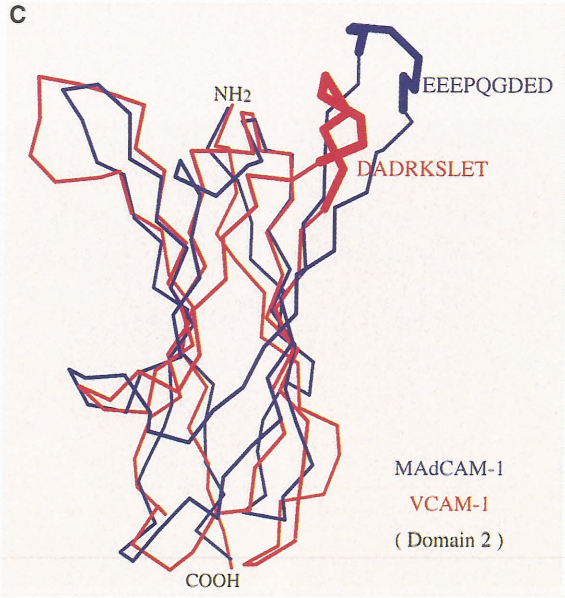

CELL ADHESION & COMMUNICATION VOLUME 7, NUMBER 3.
COLOR PLATE I. See N. GREEN *et al.*, Figure 1(C).

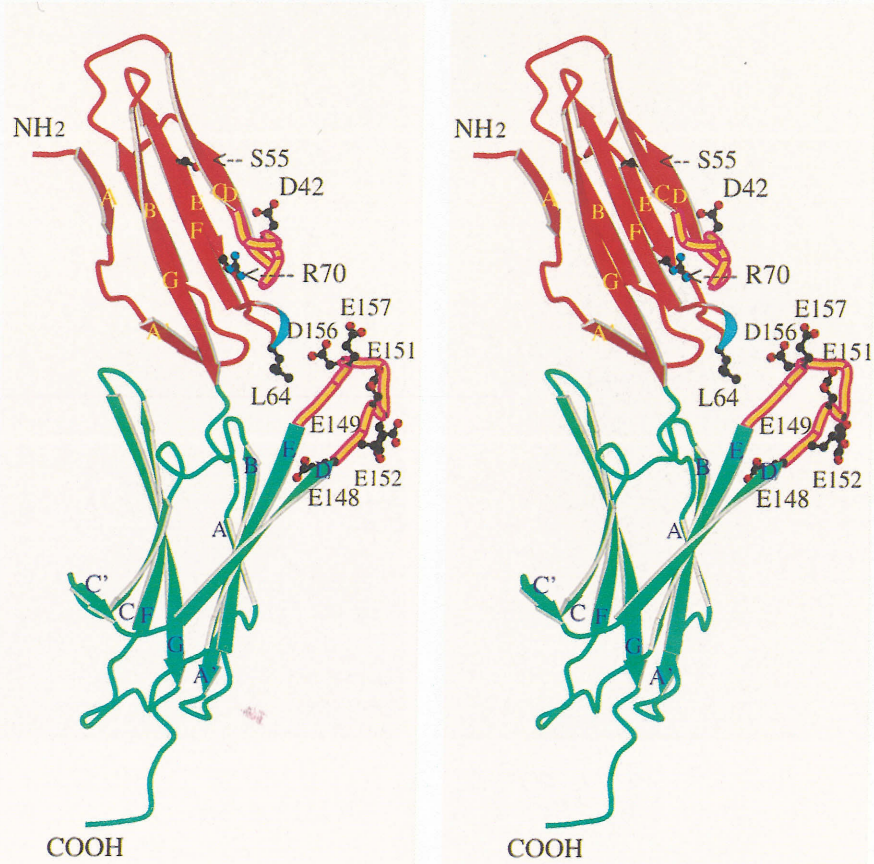

CELL ADHESION & COMMUNICATION VOLUME 7, NUMBER 3.
COLOR PLATE II. See N. GREEN *et al.*, Figure 4.

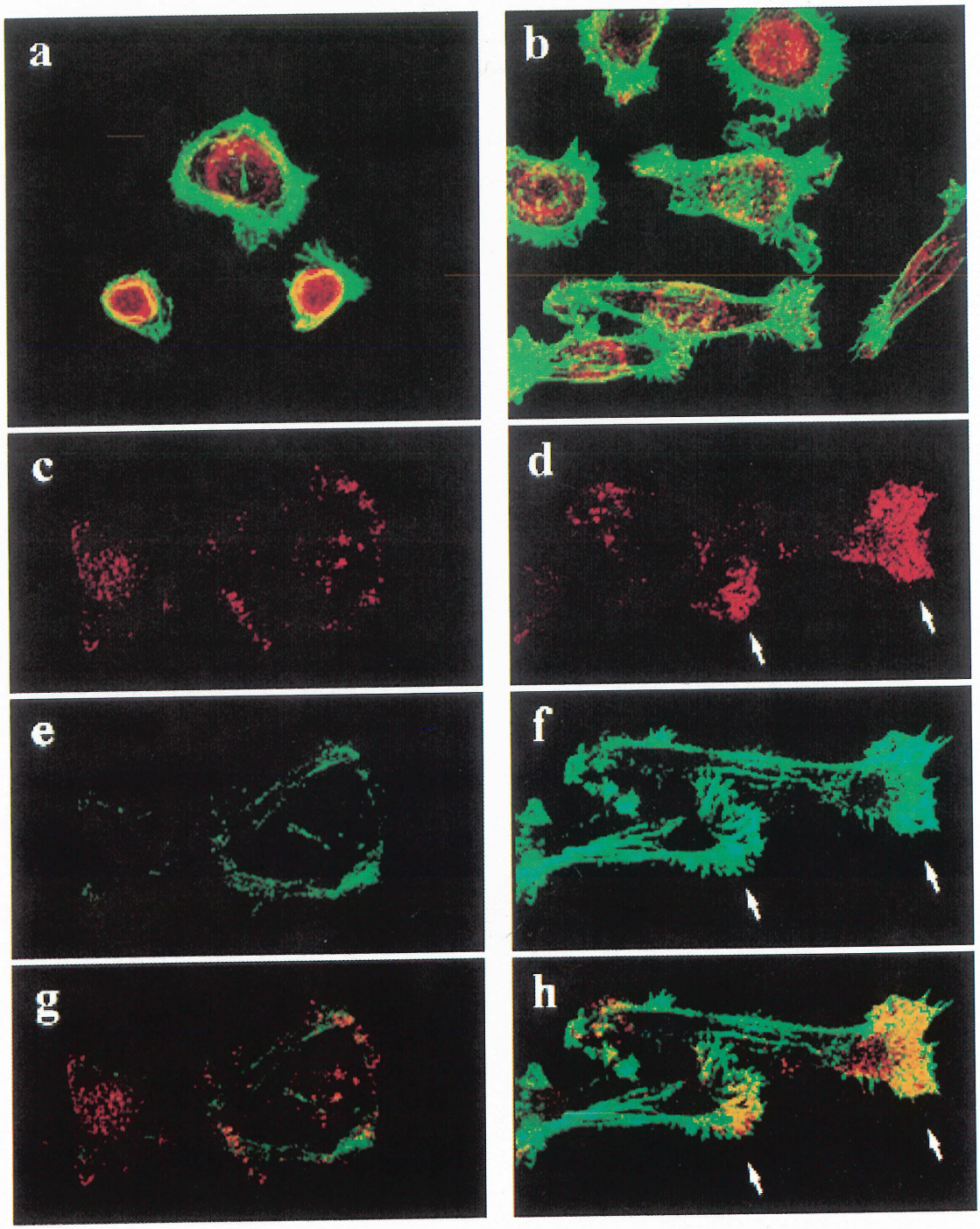

CELL ADHESION & COMMUNICATION VOLUME 7, NUMBER 3.
COLOR PLATE III. See E.E. PUTNINS *et al.*, Figure 5.